AGU PUBLICATIONS

Geophysical Research Letters

RESEARCH LETTER
10.1002/2017GL074470

Key Points:
- The MJO phase with convection in the West Pacific precedes a weaker vortex in two subseasonal forecast models
- Time scale of predictability for SSW events may approach 4 weeks if a strong MJO event is realistically simulated
- Ensemble spread in stratospheric circulation is related to ensemble spread in tropical convection

Supporting Information:
- Supporting Information S1

Correspondence to:
C. I. Garfinkel,
chaim.garfinkel@mail.huji.ac.il

Citation:
Garfinkel, C. I., & Schwartz, C. (2017). MJO-related tropical convection anomalies lead to more accurate stratospheric vortex variability in subseasonal forecast models. *Geophysical Research Letters*, *44*, 10,054–10,062. https://doi.org/10.1002/2017GL074470

Received 6 JUN 2017
Accepted 9 SEP 2017
Accepted article online 14 SEP 2017
Published online 13 OCT 2017

MJO-Related Tropical Convection Anomalies Lead to More Accurate Stratospheric Vortex Variability in Subseasonal Forecast Models

C. I. Garfinkel[1] **and C. Schwartz**[1]

[1] Fredy and Nadine Hartmann Institute of Earth Sciences, Hebrew University, Jerusalem, Israel

Abstract The effect of the Madden-Julian Oscillation (MJO) on the Northern Hemisphere wintertime stratospheric polar vortex in the period preceding stratospheric sudden warmings is evaluated in operational subseasonal forecasting models. Reforecasts which simulate stronger MJO-related convection in the Tropical West Pacific also simulate enhanced heat flux in the lowermost stratosphere and a more realistic vortex evolution. The time scale on which vortex predictability is enhanced lies between 2 and 4 weeks for nearly all cases. Those stratospheric sudden warmings that were preceded by a strong MJO event are more predictable at ~20 day leads than stratospheric sudden warmings not preceded by a MJO event. Hence, knowledge of the MJO can contribute to enhanced predictability, at least in a probabilistic sense, of the Northern Hemisphere polar stratosphere.

Plain Language Summary Atmospheric variability in the polar stratosphere, the atmospheric layer between approximately 10 km and 50 km above the surface, strongly impacts surface climate over the eastern United States and Eurasia. It is thought that variability in this region can be predicted up to 15 days in advance. Here we show that knowledge of the state of convection in the tropical Pacific and Indian Ocean can lead to enhanced predictability up to 4 weeks in advance.

1. Introduction

Variability of the Northern Hemisphere wintertime stratospheric polar vortex can influence tropospheric weather and climate (Baldwin & Dunkerton, 1999; Limpasuvan et al., 2004; Polvani & Kushner, 2002). An anomalously weak vortex can lead to the negative phase of the Northern Annular Mode (also known as the Arctic Oscillation) in the weeks or months following an event (Baldwin & Dunkerton, 2001; Limpasuvan et al., 2004; Polvani & Waugh, 2004), while an anomalously strong vortex has largely opposite impacts (Limpasuvan et al., 2005). It is therefore important to understand the time scale over which intraseasonal variability of the polar vortex can be predicted, in order to lead to more skillful subseasonal forecasts.

Numerical Weather Prediction (NWP) models simulate longer predictability in the stratosphere in comparison to that in the troposphere. For example, Jung and Leutbecher (2007) and Zhang et al. (2013) showed that forecast skill in the NH extratropical stratosphere is roughly twice that of the troposphere for the same forecast lead time. This skill is mostly linked to the ability to represent anomalies in the zonal mean circulation, even if models are unable to skilfully forecast the planetary waves whose fluxes ultimately drive the zonal mean circulation.

However, stratospheric predictability is lowest in the leadup to stratospheric sudden warming (SSW) events when strong pulses of planetary wave activity impinge on the stratosphere, leading to nonlinear interactions between waves and the mean flow that cause a reversal of the mean flow (Noguchi et al., 2016; Taguchi, 2014). The predictability of SSW events is generally between 5 and 15 days (Tripathi et al., 2015), no better than that of tropospheric weather systems. Tripathi et al. (2016) found that the onset of the January 2013 SSW was well predicted for lead times of up to 10 days in initialized NWP systems, but the predictability was significantly diminished for lead times of 15 days.

It is well known that tropical diabatic heating associated with the Madden-Julian Oscillation (MJO), the dominant mode of intraseasonal variability in the tropics (Madden & Julian, 1994), excites subtropical planetary waves via barotropic vorticity perturbations which then propagate poleward (Ferranti et al., 1990; Gill, 1980;

Lukens et al., 2017; Seo & Son, 2012; Weare et al., 2012). These wave perturbations are known to influence northern hemispheric weather patterns in the troposphere (Cassou, 2008; Johnson & Feldstein, 2010; L'Heureux & Higgins, 2008; Lin et al., 2009; Riddle et al., 2013; Yoo et al., 2012).

Recently, Garfinkel et al. (2012, 2014) found that this poleward propagating wave train of the MJO can propagate upward into the stratosphere and modulate stratospheric temperatures. About 10 days after the MJO passes its phase with enhanced (reduced) convection over the central Pacific (Indian) Ocean (phase 7 as defined by Wheeler and Hendon (2004)), warm anomalies are established in the polar lower stratosphere. This warming is driven by constructive interference between the midlatitude circulation anomaly generated by the anomalous MJO convection and the climatological stationary wave pattern (e.g., Figures 9 and 11 of Goss et al., 2016). In contrast, anomalous cooling occurs in the stratosphere about 10 days after MJO phase 4, which has convective anomalies largely of opposite sign to that of phase 7. A similar response was also evident in the model experiments examined by Garfinkel et al. (2014) and by Kang and Tziperman (2017), and in the analysis of Liu et al. (2014). Newman and Sardeshmukh (2008) also demonstrated that intraseasonal variability in tropical heating can affect the stratospheric polar vortex.

The goal of this work is to consider whether models used in operational subseasonal forecasting can capture this association between the MJO and stratospheric variability and to consider whether this association can lead to enhanced predictability of stratospheric variability beyond 15 days. We demonstrate that reforecast ensemble members which simulate deeper convection in the tropical west Pacific/maritime continent shortly after forecast initiation also simulate a weaker vortex, and in some cases a SSW. We also show that SSW events preceded by a MJO phase 6/7 event are more predictable than those SSW events not preceded by a MJO phase 6/7 event.

2. Data and Methods

The association between MJO-related outgoing longwave radiation (OLR) anomalies and stratospheric variability is examined in models that have contributed to the Subseasonal to Seasonal (S2S) Prediction research project database (Vitart et al., 2017). As the results of this study are based in large part on analyzing intraensemble diversity, we examine models which archive at least 11 ensemble members for each reforecast. Three models meet these criteria—the Australian Bureau of Meteorology (BoM), the European Centre for Medium-Range Weather Forecasts (ECMWF), and Météo-France/Centre National de Recherche Meteorologiques (CNRM)—but only the first two are included as the CNRM has made available only two reforecasts available per month and thus the temporal resolution is not sufficient to fully capture the leadup to specific SSW events. The ECMWF has made available 11 ensemble members, while BoM has made available 33 (11 from each of 3 model versions). We assume only 11 independent degrees of freedom for each BoM reforecast ensemble for reasons discussed in the supporting information. Note that the BoM model has a model top at 10 hPa.

We focus on those SSW events which were preceded by a phase 6/7 of the MJO as defined by the Real-time Multivariate (RMM) MJO index (Wheeler & Hendon, 2004). Schwartz and Garfinkel (2017) identify 12 SSW events (out of 23 since 1979 using the definition of Butler et al. (2014)) as having been preceded by a strong MJO phase 6 or 7. Of the 12 events identified by Schwartz and Garfinkel (2017), 11 occurred after the start date for BoM reforecasts and 8 occurred after the start date for ECMWF reforecasts. Here we examine reforecasts that were initialized at least 2 weeks before each of these 11 BoM cases and 8 ECMWF cases. Section 4 compares the predictability of these SSW with the 10 SSWs that have occurred after the start date for BoM reforecasts without a preceding MJO phase 6/7 event.

For each SSW event, we go backward in time from the BoM reforecast initialized at least 2 weeks before the SSW and identify the earliest BoM reforecast that captures qualitatively the relationship between MJO-related tropical convection and polar stratospheric variability (i.e., integrations with a stronger MJO-related convection simulate a weaker vortex). MJO-related tropical convection is indexed by OLR in the west Pacific (120°E to 150°E, 0–10°N). We elect to focus on OLR in this region as MJO-related convective anomalies are strong in this longitude band for MJO phase 6. We focus on convection north of the equator only as we found a stronger connection to the NH extratropical stratosphere if we limited our focus to convection north of the equator (not shown). In addition, Schwartz and Garfinkel (2017) found that convective variability in this region precedes tropospheric anomalies in the subpolar northwest Pacific where anomalies can efficiently lead to constructive or destructive interference with the climatological planetary waves, while convective variability to the

Table 1
Initialization Dates and Lag at Which We Examine OLR in the West Pacific for Each SSW

	BoM		ECMWF	
SSW date	Initialization date	OLR lags	Initialization date	OLR lags
2-Jan-1985	16-Dec-1984	9 to 17		
8-Dec-1987	16-Nov-1987	2 to 12		
22-Feb-1989	6-Feb-1989	1 to 6		
15-Dec-1998	26-Nov-1998	3 to 17	28-Nov-1998	1 to 15
25-Feb-1999	6-Feb-1999	3 to 11	4-Feb-1999	5 to 13
2-Jan-2002	11-Dec-2001	3 to 12	8-Dec-2001	10 to 25
18-Jan-2003	1-Jan-2003	9 to 14	2-Jan-2003	8 to 13
7-Jan-2004	21-Dec-2003	5 to 11	19-Dec-2003	7 to 13
22-Feb-2008	6-Feb-2008	5 to 10	6-Feb-2008	5 to 10
24-Jan-2009	6-Jan-2009	7 to 13	5-Jan-2009	8 to 14
9-Feb-2010	16-Jan-2010	4 to 15	16-Jan-2010	4 to 15

Note. ECMWF reforecasts are not available in the 1980s. For all events except the SSW on 2 Jan 2002 we select the same calendar dates for both BoM and ECMWF. For this event the MJO was a strong phase 6/7 (except a brief excursion to phase 8) for nearly four consecutive weeks (Weickmann & Berry, 2007), and the apparent connection between this stalled MJO event and the stratosphere appears to operate at different lags between BoM and ECMWF for reasons beyond the scope of this work.

south of this region or its immediate east (i.e., where the enhanced convection during MJO phase 7 peaks) has relatively little effect on the subpolar northwest Pacific response. Because of the peculiarities of each MJO event and differences in the date on which each reforecast was initialized as compared to the start date for each MJO event, we select OLR at different lags for each reforecast that match the specific MJO event, though in many cases we shift the start or end date of the period chosen by several days in order to better capture the connection between convective anomalies and the stratosphere. The forecast initialization date and the lags chosen for each SSW event are listed in Table 1. We then pick the corresponding reforecast from the ECMWF.

Our next step is to examine 100 hPa heat flux area averaged from 40°N to 80°N for zonal wave numbers 1 and 2 lagged 6 days from the period chosen for the west Pacific OLR (e.g., if OLR is examined from day 5 to 10 of a given reforecast, we examine heat flux from day 11 to 16)—results are similar for a lag of 5 or 7 days. Garfinkel et al. (2014) showed that positive heat flux anomalies occur simultaneously with phase 7 in the troposphere and in the 10 days after phase 7 in the stratosphere, motivating our choice of 6 days for our phase 6/7 composite. Note that the heat flux is proportional to the vertical component of the Eliassen-Palm flux and hence is a proxy for wave activity in the lower stratosphere and subsequent stratospheric variability (e.g., Newman et al., 2001). Results are slightly weaker if we focus on the total heat flux (i.e., all zonal wave numbers). For some events the heat flux window extends past the central date for the SSW, and it is well known that heat flux at 100 hPa weakens significantly following SSW events (Limpasuvan et al., 2004) due to internal stratospheric processes (Holton & Mass, 1976). In order to maintain focus on the stratospheric evolution leading up to the SSW, these days after the SSW central date are removed from the heat flux composite. We then consider the polar stratospheric state from 1 day before to 1 day after the observed SSW occurred using two metrics: 70°N and poleward area-weighted averaged geopotential height at 10 hPa, and zonal wind at 10 hPa and 60°N.

3. Importance of West Pacific Convection for Intraensemble Spread

We begin with a case study of the SSW event that occurred on 2 January 2002 (based on zonal wind reversal at 60°N and 10 hPa in NCEP). This SSW was preceded by a strong MJO event that crossed from phase 5 to phase 6 on 8 December 2001 (as defined by Wheeler and Hendon (2004)) and maintained an RMM amplitude above 1.0 in phases 6 and 7, with a brief excursion to 8, until the SSW. The tropical dynamics associated with this event, including possible causes of its prolonged period of enhanced west Pacific convection, are discussed by Weickmann and Berry (2007). The representation of this event in reforecasts initialized on 8 December 2001 from ECMWF is shown in Figure 1. The reforecasts are composited into two groups based on OLR in the west Pacific (120°E to 150°E, 0–10°N) over day 10 to 25 of the reforecast, in which the three integrations with the highest OLR values are composited together (green), and the three integrations with the lowest OLR are

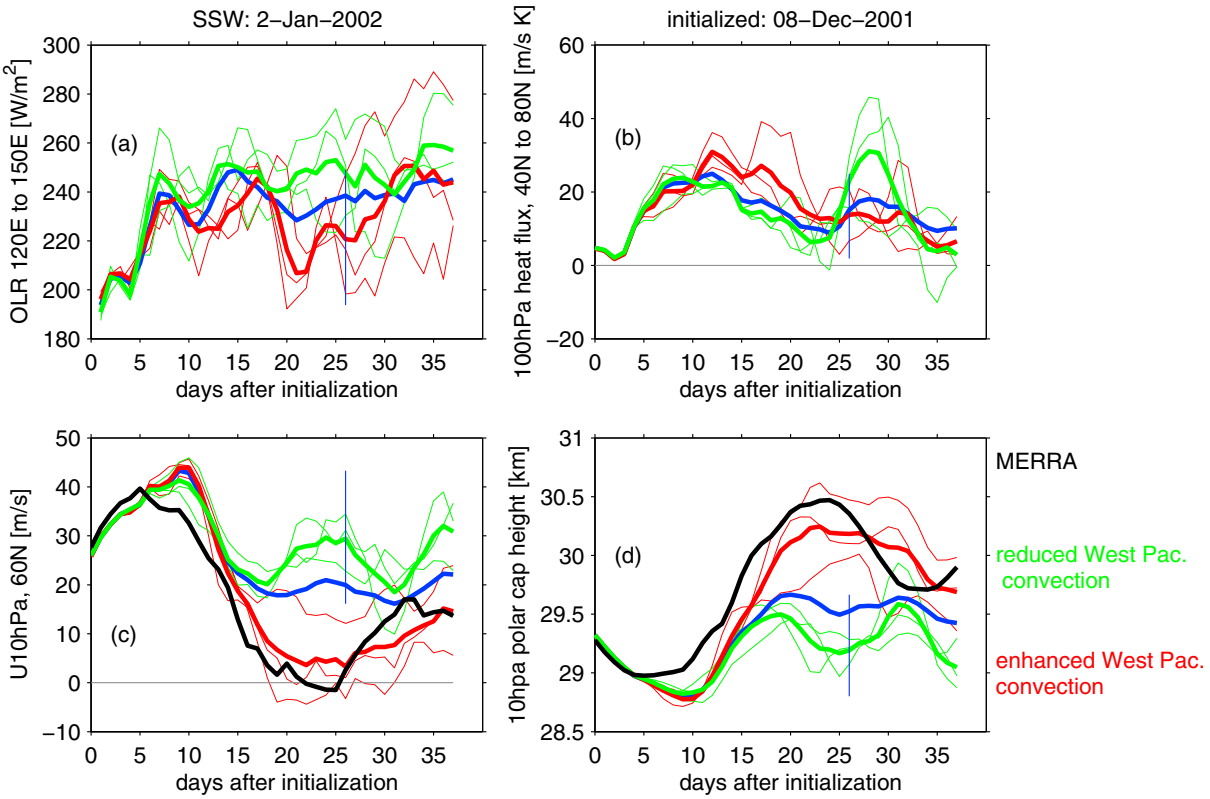

Figure 1. Connection between the MJO and stratospheric circulation in the ECMWF in reforecasts initialized on 8 December 2001. The reforecasts are divided into three groups based on OLR in the west Pacific (120°E to 150°E, 0–10°N) over days 10 to 25 of the reforecast. The first group is the three integrations with the highest OLR values (green), the second group is the three integrations with the lowest OLR values (red), and all other integrations are included in the third group. The evolution of (a) OLR in the west Pacific, (b) zonal wave number 1 + 2 heat flux area averaged from 40°N to 80°N, (c) zonal wind at 10 hPa, 60°N, and (d) polar cap height area weighted from 70°N and poleward at 10 hPa. Black lines in Figures 1c and 1d are for the Modern-Era Retrospective Analysis for Research and Application (MERRA) reanalysis. Individual integrations are shown with thin lines, and a thick blue line denotes the ensemble mean for all integrations initialized on 8 December 2001. A thin vertical blue line indicates the day of the SSW using National Centers for Environmental Prediction (NCEP) data.

composited together (red). Integrations without large deviations in OLR are not included in either group, and results are not sensitive to compositing the, for example, two or four most extreme integrations. Figure 1a shows the composite evolution of outgoing longwave radiation (OLR) for the month after initialization for these integrations, and the ensemble-mean evolution is shown in blue. These groups of integrations show different upward propagating wave flux entering the stratosphere (Figure 1b), which is proportional to the northward sensible heat flux: Heat fluxes from lag 10 to lag 25 days are larger for those integrations with lower OLR. The enhanced wave flux modulates stratospheric winds and geopotential height approximately 5 days later. Figure 1c shows that zonal winds at 10 hPa and 60°N are weaker (i.e., relatively easterly) in the experiments with low OLR (enhanced convection) in the west Pacific as compared to the high OLR composite. Similar sensitivity is also seen in Figure 1d: Polar cap heights are higher in the reforecasts with lower OLR in the west Pacific. Two of the ensemble members simulate a SSW for an initialization date 26 days before the actual SSW, and both of these belong to the composite of integrations with the lowest OLR (more convection) in the west Pacific (thin red lines).

A similar analysis has been performed for the other SSW events listed in Table 1, and figures comparable to Figure 1 but for four of these case studies (22 February 1989 and 15 December 1998 for BoM and 7 January 2004 and 9 February 2010 for ECMWF) are shown in the supporting information.

Figures 2 and 3 summarize the results across all case studies. Figure 2 suggests that the MJO can be used to inform a probabilistic forecast of stratospheric variability. Figure 2 (top row) shows a probability distribution function (PDF) of 100 hPa heat flux lagged by 6 days constructed separately for those integrations with enhanced and reduced convection in the west Pacific. In both models, integrations with enhanced convection are followed by enhanced heat fluxes at 100 hPa, and the difference between the two PDFs is statistically

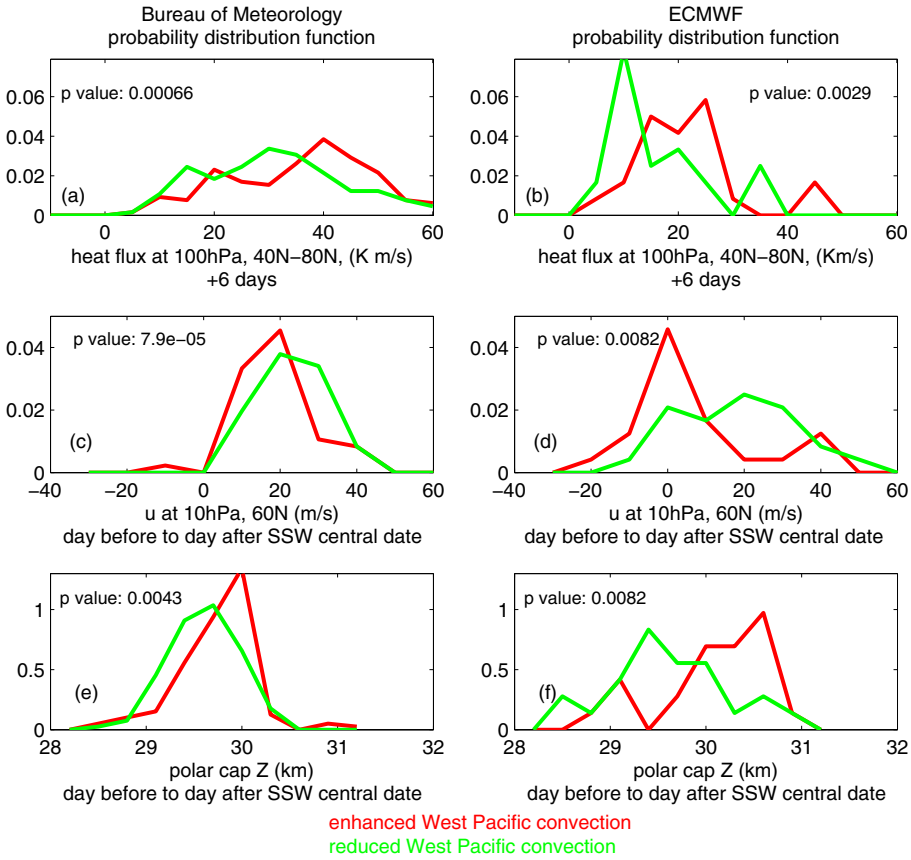

Figure 2. The probability distribution function of the extratropical stratospheric state following anomalous convection in the west Pacific. A green line indicates the 3 (12) integrations with the highest OLR values in the west Pacific in ECMWF (BoM), while a red line indicates the 3 (12) integrations with the lowest OLR values in the west Pacific in ECMWF (BOM), for each event listed in Table 1. (top row) Midlatitude zonal wave number 1 + 2 heat flux entering the stratosphere lagged 5 days after the convective anomalies, (middle row) zonal wind at 10 hPa, 60°N on the 3 days surrounding the SSW central date, and (bottom row) polar cap height area weighted from 70°N and poleward at 10 hPa on the 3 days surrounding the SSW central date. Each panel lists the *p* value for the difference between the two PDFs using a Kolmogorov-Smirnov test.

significant using a Kolmogorov-Smirnov test. Similar results are obtained for both zonal wind at 10 hPa, 60°N (middle row) and polar cap geopotential height (bottom row), and in all cases the PDFs are significantly different from each other. Hence, it is clear that anomalies in tropical convection lead stratospheric variability, with integrations simulating enhanced west Pacific convection also simulating more realistic stratospheric variability.

A second way to summarize the results across all case studies is shown in Figure 3. For each reforecast date, we compute the correlation between OLR in the west Pacific and 100 hPa heat flux lagged 6 days across all 33 (for BoM) or 11 integrations (for ECMWF). We display the correlation for each integration in Figure 3a. The lagged correlations are negative for nearly all SSW events, whereby integrations with lower OLR are associated with stronger 100 hPa midlatitude heat flux. (Note that BoM fails to capture the relationship between convection and the very strong SSW on 24 January 2009 for a start date of 6 January. It does succeed in capturing the relationship for a start date of 11 January, though in this paper we intentionally focus on reforecasts initialized at least 2 weeks before the SSW). While the correlations for individual SSW events are not statistically significant likely due to the limited sample size, the correlation across all SSW events is statistically significant at the 95% level (indicated with a large black "x" in Figure 3).

Figure 3b considers the correlation between OLR variability and zonal wind at 10 hPa, 60°N on the 3 days surrounding the observed SSW. As for heat flux, there is a close relationship between MJO-related convection and stratospheric variability. Figure 3c shows that this relationship is present for polar cap geopotential height

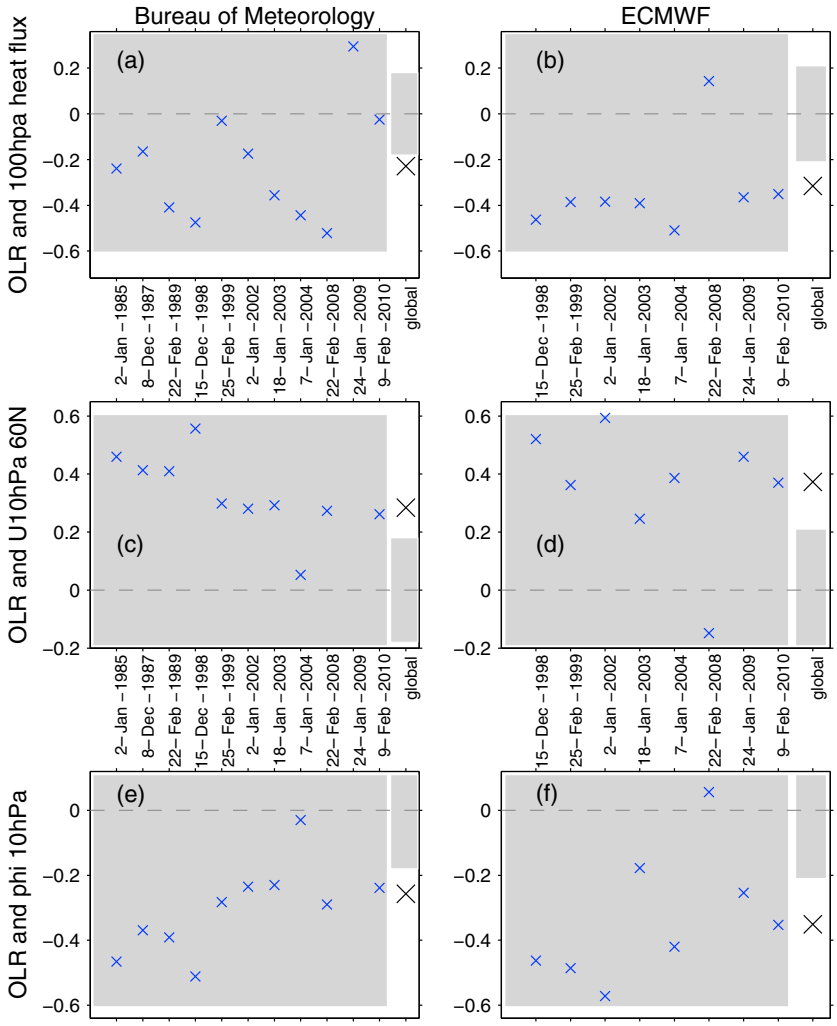

Figure 3. Summary of the relationship between MJO and SSW for all reforecasts considered by this paper. Correlation across all integrations between OLR in the west Pacific and (a, b) 100 hPa zonal wave number 1 + 2 heat flux lagged 6 days; (c, d) zonal wind at 10 hPa, 60°N on the 3 days surrounding the observed SSW; (e, f) polar cap geopotential height at 10 hPa. Gray shading indicates the region in which results are not statistically significant for assuming 11 independent degrees of freedom for each reforecast ensemble (as discussed in the supporting information). The black x represents the correlation across all events.

at 10 hPa as well. Similar results are evident for the ECMWF reforecasts as well: Reforecasts in which OLR is lower over the west Pacific subsequently simulate a weaker stratospheric vortex. While this effect is not statistically significant for individual SSW events, it is statistically significant over the entire composite of events. The net effect is that tropical convection leads to NH polar stratospheric variability.

4. Enhanced Predictability for SSW Preceded by a Strong MJO

Thus far we have shown that intraensemble variability in convection explains a significant fraction of the ensemble spread in vortex state. We now consider a related question: Are SSW that were preceded by phase 6/7 of the MJO more predictable at ~20 day leads than those SSW without any preceding MJO activity? To answer this question, we compare predictability in the extratropical circulation for the SSW considered thus far in BoM to extratropical variability in the BoM reforecasts for SSW events that were not preceded by a phase 6/7 MJO event (listed in Table 1 of Schwartz and Garfinkel (2017)). We only include SSW events that occurred after 1981 (i.e., the start date for BoM reforecasts). For SSW preceded by a phase 6/7 MJO event we choose the initialization dates listed in Table 1: The mean initialization date is 19.8 days. For SSW not preceded by a phase 6/7 MJO event, we choose reforecasts initialized 18 and 22 days before the SSW in order to focus on similar lags, and the mean initialization date is 19.3 days.

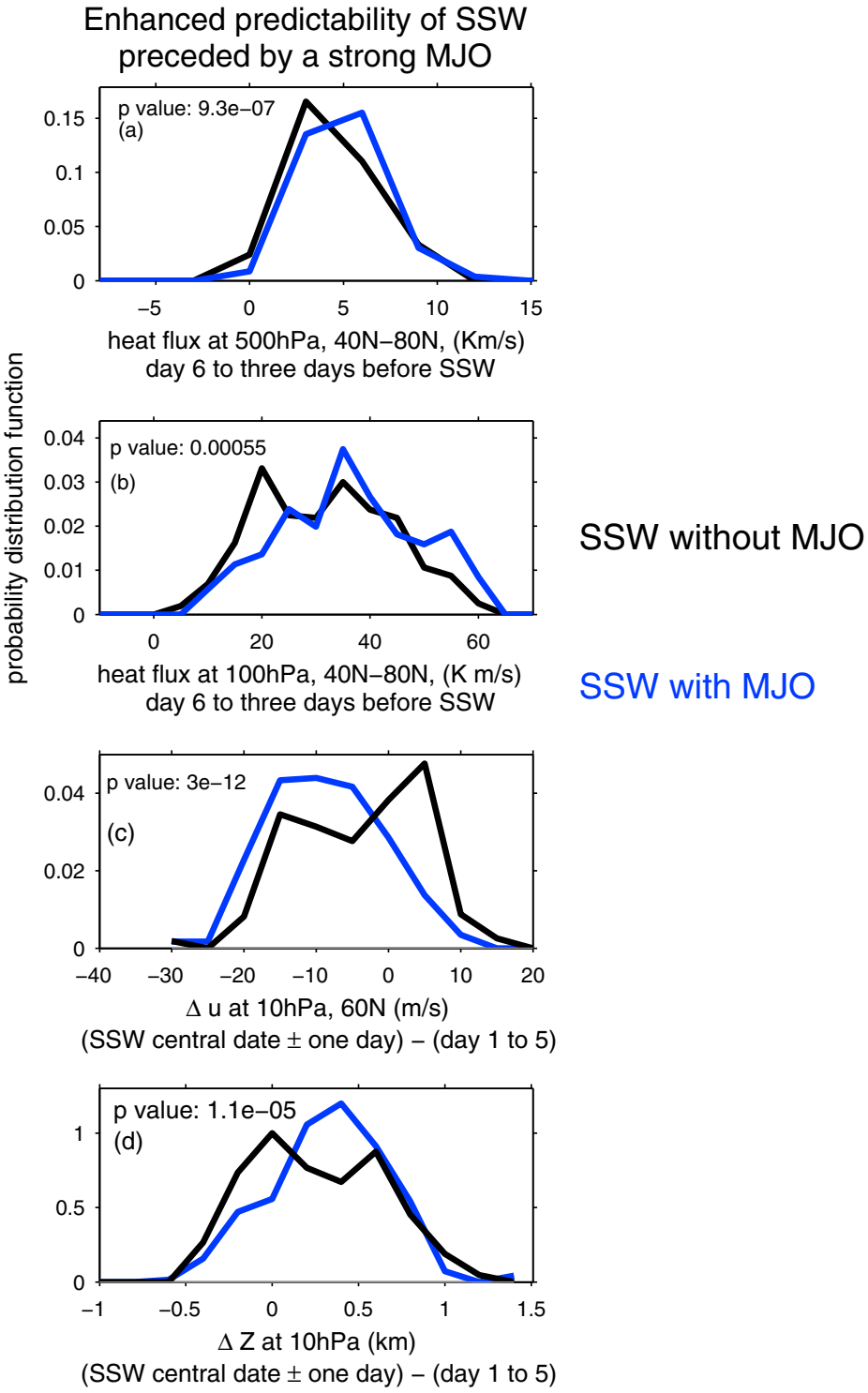

Figure 4. Probability distribution functions of extratropical variability preceding SSW events in the BoM reforecast ensemble, stratified by whether the SSW was preceded by phase 6/7 of the MJO or not as given by Table 1 of Schwartz and Garfinkel (2017). Only SSW events which occurred after 1981 are included, which leads to 10 SSW events not preceded by phase 6/7 of the MJO (black) and 11 SSW events preceded by phase 6/7 of the MJO (blue): (a) 500 hPa zonal wave number 1 + 2 heat flux 6 days after initialization to 3 days before the SSW central date; (b) as in Figure 4a but for 100 hPa wave number 1 + 2 heat flux; (c) the change in zonal wind at 10 hPa, 60°N between the 3 days surrounding the observed SSW and days 1 to 5 of the reforecast; (d) as in Figure 4c but for geopotential height at 10 hPa area weighted from 70°N and poleward. Each panel lists the *p* value for the difference between the two PDFs using a Kolmogorov-Smirnov test.

Figure 4a compares the probability distribution function of 500 hPa zonal wave number 1 + 2 heat flux 6 days after initialization to 3 days before the SSW central date (results are not sensitive to the precise time period chosen). Tropospheric planetary wave activity is significantly stronger for SSW events that were preceded by phase 6/7 of the MJO as compared to those SSW events without phase 6/7 of the MJO. This significant difference in tropospheric planetary waves extends into the stratosphere (Figure 4b). Figure 4c shows the PDF of the change in zonal wind at 10 hPa, 60°N between the 3 days surrounding the observed SSW and days 1 to 5 of the reforecast; the vortex weakens in more than 85% of the reforecasts initialized ~20 days before SSW events that were preceded by phase 6/7 of the MJO. In contrast, only 60% of the reforecasts of SSW without phase 6/7 of the MJO show weakening of the vortex. Similar results are evident for polar cap geopotential height at 10 hPa (Figure 4d). The difference in the PDFs in all four panels of Figure 4 is highly statistically significant. Overall, SSW events that were preceded by phase 6/7 of the MJO are more predictable at ~20 day leads as compared to SSW events not preceded by phase 6/7 of the MJO.

5. Summary

Stratospheric variability has important implications for surface climate (Baldwin & Dunkerton, 1999; Limpasuvan et al., 2004; Polvani & Kushner, 2002), and hence, it is crucial to understand the time scale over which stratospheric variability can be predicted. Here we have examined whether tropical convective anomalies associated with the MJO modulate stratospheric variability in operational subseasonal forecasting models, and to consider the duration over which this association can potentially lead to enhanced predictability of stratospheric variability at least in a probabilistic sense. For two different operational models and for nearly all SSW events, reforecasts which maintain anomalously strong MJO-related convection simulate more realistic stratospheric variability up to 4 weeks later. Furthermore, stratospheric variability is more predictable for SSW events that were preceded by a phase 6/7 MJO event as compared to SSW events not preceded by a strong MJO event.

It is interesting to note that the BoM model has a model top at 10 hPa yet is still capable of capturing the relationship between the MJO and SSWs (as in the low-top model considered by Garfinkel et al. (2014)). However, the BoM model struggles to capture SSW (cf. Figure 2), similar to the low-top models contributed to the Coupled Model Intercomparison Project phase 5 (Charlton-Perez et al., 2013). Furthermore, we note that in Figure 4, the BoM model captures weakening of the vortex over the 20 day period preceding a SSW even for SSW events not preceded by a strong MJO, though the weakening is significantly larger for SSW that were preceded by a strong MJO. This suggests that weakening of the stratospheric vortex may be predictable in a probabilistic sense even without anomalous MJO conditions.

We note the caveat that while reforecasts with strong MJO-related convection simulate stratospheric variability closer to reality, the reforecasts examined in this study generally do not simulate an SSW: Only the tail of the probability distribution function for enhanced convection in Figure 2c extends to negative zonal wind values at 10 hPa, 60°N. Second, we have not yet addressed whether knowledge of a developing MJO actually contributes skill toward forecasting a SSW, though we plan to explore this question for future work. However, results of this work, combined with that of Garfinkel et al. (2012), Liu et al. (2014), and Garfinkel et al. (2014), suggest the potential for predictability of SSW events at least in a probabilistic sense up to 4 weeks in advance given that the evolution of the MJO can be predicted with some skill up to a few weeks (Marshall et al., 2016; Vitart, 2017).

Acknowledgments

C. I. G. and C. S. were supported by the Israel Science Foundation (grant 1558/14) and by a European Research Council starting grant under the European Unions Horizon 2020 research and innovation programme (grant agreement 677756). The authors thank the two anonymous reviewers for their helpful comments which led to an improved manuscript. This work is based on S2S data. S2S is a joint initiative of the World Weather Research Programme (WWRP) and the World Climate Research Programme (WCRP). The original S2S database is hosted at ECMWF as an extension of the TIGGE database and can be downloaded from the ECMWF server http://apps.ecmwf.int/datasets/data/s2s/levtype=sfc/type=cf/. The real-time multivariate index of Wheeler and Hendon (2004) was downloaded from the BoM website (http://www.bom.gov.au/climate/mjo/graphics/rmm.74toRealtime.txt).
Correspondence and requests for data should be addressed to C. I. G. (e-mail: chaim.garfinkel@mail.huji.ac.il).

References

Baldwin, M. P., & Dunkerton, T. J. (1999). Propagation of the Arctic Oscillation from the stratosphere to the troposphere. *Journal of Geophysical Research*, *104*(D24), 30,937–30,946.

Baldwin, M. P., & Dunkerton, T. J. (2001). Stratospheric harbingers of anomalous weather regimes. *Science*, *294*(5542), 581–584.

Butler, A. H., Polvani, L. M., & Deser, C. (2014). Separating the stratospheric and tropospheric pathways of El Niño–Southern Oscillation teleconnections. *Environmental Research Letters*, *9*(2), 024014.

Cassou, C. (2008). Intraseasonal interaction between the Madden-Julian Oscillation and the North Atlantic Oscillation. *Nature*, *455*, 523–527. https://doi.org/10.1038/nature07286

Charlton-Perez, A. J., Baldwin, M. P., Birner, T., Black, R. X., Butler, A. H., Calvo, N., … Watanabe, S. (2013). On the lack of stratospheric dynamical variability in low-top versions of the CMIP5 models. *Journal of Geophysical Research: Atmospheres*, *118*, 2494–2505. https://doi.org/10.1002/jgrd.50125

Ferranti, L., Palmer, T., Molteni, F., & Klinker, E. (1990). Tropical-extratropical interaction associated with the 30–60 day oscillation and its impact on medium and extended range prediction. *Journal of the Atmospheric Sciences*, *47*(18), 2177–2199.

Garfinkel, C. I., Benedict, J. J., & Maloney, E. D. (2014). Impact of the MJO on the boreal winter extratropical circulation vortex. *Geophysical Research Letters*, *41*, 6055–6062. https://doi.org/10.1029/2014GL061094

Garfinkel, C. I., Feldstein, S. B., Waugh, D. W., Yoo, C., & Lee, S. (2012). Observed connection between stratospheric sudden warmings and the Madden-Julian oscillation. *Geophysical Research Letters*, *39*, L18807. https://doi.org/10.1029/2012GL053144

Gill, A. E. (1980). Some simple solutions for heat-induced tropical circulation. *Quarterly Journal of the Royal Meteorological Society*, *106*, 447–462. https://doi.org/10.1002/qj.49710644905

Goss, M., Feldstein, S. B., & Lee, S. (2016). Stationary wave interference and its relation to tropical convection and arctic warming. *Journal of Climate*, *29*(4), 1369–1389.

Holton, J. R., & Mass, C. (1976). Stratospheric vacillation cycles. *Journal of Atmospheric Science*, *33*, 2218–2225.

Johnson, N. C., & Feldstein, S. B. (2010). The continuum of North Pacific sea level pressure patterns: Intraseasonal, interannual, and interdecadal variability. *Journal of Climate*, *23*, 851–867. https://doi.org/10.1175/2009JCLI3099.1

Jung, T., & Leutbecher, M. (2007). Performance of the ECMWF forecasting system in the Arctic during winter. *Quarterly Journal of the Royal Meteorological Society*, *133*(626), 1327–1340.

Kang, W., & Tziperman, E. (2017). More frequent sudden stratospheric warming events due to enhanced MJO forcing expected in a warmer climate. *Journal of Climate*, *30*, 8727–8743. https://doi.org/10.1175/JCLI-D-17-0044.1

L'Heureux, M. L., & Higgins, R. W. (2008). Boreal winter links between the Madden–Julian Oscillation and the Arctic Oscillation. *Journal of Climate*, *21*, 3040–3050. https://doi.org/10.1175/2007JCLI1955.1

Limpasuvan, V., Hartmann, D. L., Thompson, D. W. J., Jeev, K., & Yung, Y. L. (2005). Stratosphere-troposphere evolution during polar vortex intensification. *Journal of Geophysical Research*, *110*, D24101. https://doi.org/10.1029/2005JD006302

Limpasuvan, V., Thompson, D. W. J., & Hartmann, D. L. (2004). The life cycle of the Northern Hemisphere sudden stratospheric warmings. *Journal of Climate*, *17*, 2584–2596.

Lin, H., Brunet, G., & Derome, J. (2009). An observed connection between the North Atlantic Oscillation and the Madden-Julian Oscillation. *Journal of Climate*, *22*, 364–380. https://doi.org/10.1175/2008JCLI2515.1

Liu, C., Tian, B., Li, K.-F., Manney, G. L., Livesey, N. J., Yung, Y. L., & Waliser, D. E. (2014). Northern Hemisphere mid-winter vortex-displacement and vortex-split stratospheric sudden warmings: Influence of the Madden-Julian Oscillation and quasi-biennial oscillation. *Journal of Geophysical Research: Atmospheres*, *119*, 12,599–12,620. https://doi.org/10.1002/2014JD021876

Lukens, K. E., Feldstein, S. B., Yoo, C., & Lee, S. (2017). The dynamics of the extratropical response to Madden-Julian Oscillation convection. *Quarterly Journal of the Royal Meteorological Society*, *143*, 607–1184. https://doi.org/10.1002/qj.2993

Madden, R. A., & Julian, P. R. (1994). Observations of the 40–50-day tropical oscillation — A review. *Monthly Weather Review*, *122*, 814–837. https://doi.org/10.1175/1520-0493(1994)122<0814:OOTDTO>2.0.CO;2

Marshall, A. G., Hendon, H. H., & Hudson, D. (2016). Visualizing and verifying probabilistic forecasts of the Madden-Julian Oscillation. *Geophysical Research Letters*, *43*, 12,278–12,286. https://doi.org/10.1002/2016GL071423

Newman, M., & Sardeshmukh, P. D. (2008). Tropical and stratospheric influences on extratropical short-term climate variability. *Journal of Climate*, *21*, 4326. https://doi.org/10.1175/2008JCLI2118.1

Newman, P. A., Nash, E. R., & Rosenfield, J. E. (2001). What controls the temperature of the Arctic stratosphere during the spring. *Journal of Geophysical Research*, *106*, 19,999–20,010. https://doi.org/10.1029/2000JD000061

Noguchi, S., Mukougawa, H., Kuroda, Y., Mizuta, R., Yabu, S., & Yoshimura, H. (2016). Predictability of the stratospheric polar vortex breakdown: An ensemble reforecast experiment for the splitting event in January 2009. *Journal of Geophysical Research: Atmospheres*, *121*, 3388–3404. https://doi.org/10.1002/2015JD024581

Polvani, L. M., & Kushner, P. J. (2002). Tropospheric response to stratospheric perturbations in a relatively simple general circulation model. *Geophysical Research Letters*, *29*, 1114. https://doi.org/10.129/2001GL014284

Polvani, L. M., & Waugh, D. W. (2004). Upward wave activity flux as a precursor to extreme stratospheric events and subsequent anomalous surface weather regimes. *Journal of Climate*, *17*, 3548–3554.

Riddle, E. E., Stoner, M. B., Johnson, N. C., LHeureux, M. L., Collins, D. C., & Feldstein, S. B. (2013). The impact of the MJO on clusters of wintertime circulation anomalies over the North American region. *Climate Dynamics*, *40*(7–8), 1749–1766. https://doi.org/10.1007/s00382-012-1493-y

Schwartz, C., & Garfinkel, C. I. (2017). Relative roles of the MJO and stratospheric variability in North Atlantic and European winter climate. *Journal of Geophysical Research: Atmospheres*, *122*, 4184–4201. https://doi.org/10.1002/2016JD025829

Seo, K.-H., & Son, S.-W. (2012). The global atmospheric circulation response to tropical diabatic heating associated with the Madden-Julian Oscillation during northern winter. *Journal of the Atmospheric Sciences*, *69*, 79–96. https://doi.org/10.1175/2011JAS3686.1

Taguchi, M. (2014). Stratospheric predictability: Basic characteristics in JMA 1-month hindcast experiments for 1979–2009. *Journal of the Atmospheric Sciences*, *71*, 3521–3538. https://doi.org/10.1175/JAS-D-13-0295.1

Tripathi, O. P., Baldwin, M., Charlton-Perez, A., Charron, M., Eckermann, S. D., Gerber, E., … Son, S.-W. (2015). The predictability of the extra-tropical stratosphere on monthly timescales and its impact on the skill of tropospheric forecasts. *Quarterly Journal of the Royal Meteorological Society*, *141*, 987–1003. https://doi.org/10.1002/qj.2432

Tripathi, O. P., Tripathi, O. P., Baldwin, M., Charlton-Perez, A., Charron, M., Cheung, J. C. H., … Stockdale, T. (2016). Examining the predictability of the stratospheric sudden warming of January 2013 using multiple NWP systems. *Monthly Weather Review*, *144*(5), 1935–1960.

Vitart, F. (2017). Madden-Julian Oscillation prediction and teleconnections in the S2S database. *Quarterly Journal of the Royal Meteorological Society*, *143*, 2210–2220. https://doi.org/10.1002/qj.3079

Vitart, F., Ardilouze, C., Bonet, A., Brookshaw, A., Chen, M., Codorean, C., … Zhang, L. (2017). The Subseasonal to Seasonal (S2S) prediction project database. *Bulletin of the American Meteorological Society*, *98*, 163–173. https://doi.org/10.1175/BAMS-D-16-0017.1

Weare, B. C., Cagnazzo, C., Fogli, P. G., Manzini, E., & Navarra, A. (2012). Madden-Julian Oscillation in a climate model with a well-resolved stratosphere. *Journal of Geophysical Research*, *117*, D01103. https://doi.org/10.1029/2011JD016247

Weickmann, K., & Berry, E. (2007). A synoptic–dynamic model of subseasonal atmospheric variability. *Monthly Weather Review*, *135*(2), 449–474.

Wheeler, M. C., & Hendon, H. H. (2004). An all-season real-time multivariate MJO index: Development of an index for monitoring and prediction. *Monthly Weather Review*, *132*, 1917. https://doi.org/10.1175/1520-0493(2004)132<1917:AARMMI>2.0.CO;2

Yoo, C., Lee, S., & Feldstein, S. B. (2012). Mechanisms of extratropical surface air temperature change in response to the Madden-Julian Oscillation. *Journal of Climate*, *25*(17), 5777–5790. https://doi.org/10.1175/JCLI-D-11-00566.1

Zhang, Q., Shin, C.-S., van den Dool, H., & Cai, M. (2013). CFSv2 prediction skill of stratospheric temperature anomalies. *Climate dynamics*, *41*(7-8), 2231–2249.